Short-Duration Measurements and Numerical Simulation of Heat Transfer Along the Suction Side of a Film-Cooled Gas Turbine Blade

C. Camci

T. Arts

von Karman Institute for Fluid Dynamics,
B-1640 Rhode Saint Genèse,
Belgium

This paper deals with an experimental investigation of heat transfer across the suction side of a high-pressure, film-cooled gas turbine blade and with an attempt to numerically predict this quantity both with and without film cooling. The measurements were performed in the VKI isentropic compression tube facility under well-simulated gas turbine conditions. Data measured in a stationary frame, with and without film cooling, are presented. The predictions of convective heat transfer, including streamwise curvature effects are compared with the measurements. A new approach to determine the augmented mixing lengths near the ejection holes on a highly convex wall is discussed and numerical results agree well with experimentally determined heat transfer coefficients in the presence of film cooling.

Introduction

Current trends in the aircraft gas turbine industry are in the direction of increasing turbine entry temperature and pressure ratio in order to improve the engine efficiency. However, material properties often impose a limit to these thermodynamic inlet conditions. Over the last years, one of the popular methods to overcome the high temperature operation problems has been discrete hole external film cooling.

In gas turbine engines, local wall heat flux levels are dominated by complex three-dimensional flows originating from viscous effects. The existence of complicated three-dimensional flows and their interaction in a turbine cascade has been demonstrated by several authors, e.g., Sieverding [1]. Starting from the stagnation point, very thin and laminar boundary layers start to grow up. Around the stagnation zone, both high turbulence intensities and the three-dimensional flow structure are responsible for the highest heating rates on the blades [2]. Streamwise vortices develop on both sides of the profile. Streamwise vortices develop on both sides of the profile. Along the suction side, where the flow is submitted to a strong favorable pressure gradient, amplification of the instabilities originating from the leading edge, breakdown of the streamwise vortices and hairpin eddy formation are the expected phases of a laminar to turbulent transition. The important streamwise curvature variations along this surface also affect the boundary layer development.

Several film cooling studies on turbine blades have been undertaken [3, 4]. Quantities such as adiabatic wall temperature T_{aw} and adiabatic effectiveness η, directly related to an adiabatic wall configuration, have most often been presented. Some typical stages of this approach are a detailed interpretation of convex curvature effects on the coolant film behavior [5], the effect of convex curvature on η compared with a flat-plate situation [5, 7], the rotational effects on suction-side film cooling [6]. Nevertheless, in the severe engine environment of a film-cooled airfoil, the large temperature differences existing between the mainstream and the blade surface induce a certain wall temperature pattern quite different from an adiabatic one. Considering the important spatial temperature variations due to internal cooling passages and the strongly varying heat flux distribution downstream of an ejection site, a more representative quantity is the convective het transfer coefficient h, obtained from the local wall heat flux, the mainstream recovery temperature, and the local wall temperature at a prescribed coolant temperature and blowing rate. As a matter of fact, either an experimental or numerical determination of h is essential to perform any detailed heat conduction or stress analysis.

This paper deals with the theoretical and experimental investigation of heat transfer across the suction side of a high-pressure, film-cooled gas turbine blade. Spanwise-averaged convective heat transfer coefficient distributions are measured downstream of a double row of staggered cooling holes using a transient technique. Predictions are obtained from a two-dimensional boundary layer code (STAN5), taking into account the streamwise convex curvature effect and compared with the measurements. A new approach to determine the augmented mixing lengths downstream of the ejection holes is attempted and the predictions in the presence of coolant agree quite well with the measured heat transfer data in a given range of blowing rates and temperature ratios.

Contributed by the Gas Turbine Division of The American Society of Mechanical Engineers for presentation at the 30th International Gas Turbine Conference and Exhibit, Houston, Texas, March 18–21, 1985. Manuscript received at ASME Headquarters, December 27, 1984. Paper No. 85-GT-111.
Copies will be available until December 1985.

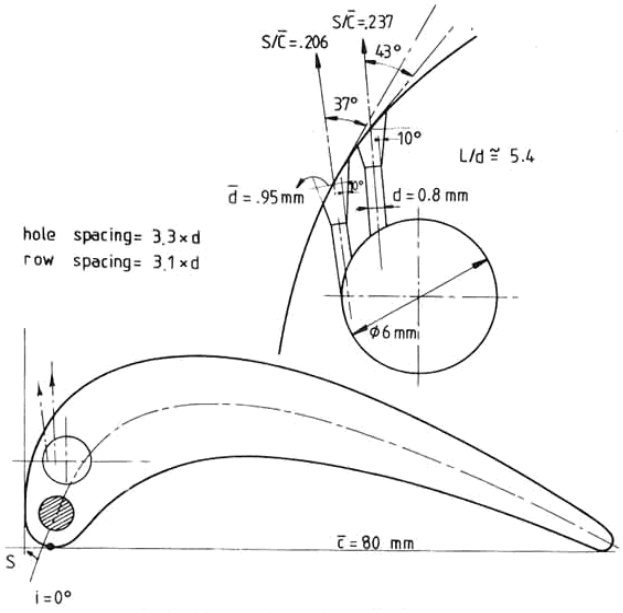

Fig. 1 Film-cooled turbine blade geometry

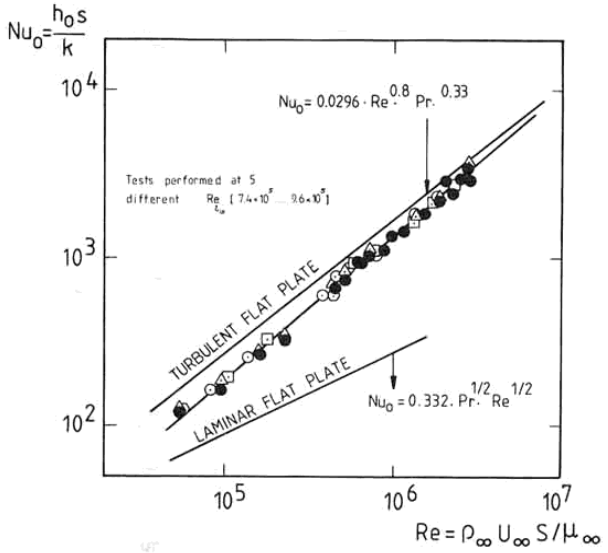

Fig. 2 Suction-side heat transfer without cooling

Experimental Apparatus

The experimental investigation was carried out in the VKI light piston isentropic compression tube facility. The same Reynolds and Mach numbers and wall to free-stream temperature ratios as encountered in actual aeroengines were generated. The coolant flow was supplied by a regenerative type cryogenic heat exchanger allowing a correct simulation of coolant to free-stream temperature ratio. The free-stream turbulence intensity was generated by a grid of parallel bars; the maximum turbulence level was 5.2 percent when the grid was installed one chord length upstream of the model [8]. Further details about this facility and its operating principles are described in [9, 10].

The coordinates of the blade and the cascade geometry were described by the authors in [13] and [8]. The local Ma number at the ejection site is 0.52. The details of measured and computed local Ma distributions were presented by the authors in [13]. The blade instrumented for heat transfer measurements was machined from a single block of low conductivity "Macor" glass ceramic and 45 platinum thin films were painted on its surface. This feature resulted in negligible conduction patterns and no artificial boundary layer disturbance, because of the smoothness of the surface. Two staggered rows of shaped holes are located on the suction side (Fig. 1). A circular cavity, drilled along the blade height, acts as a plenum. Three rows of holes are also present in the stagnation region but, for the present investigation, the leading edge plenum was filled with an insert to avoid any undesirable mainstream-plenum interaction. Pressure tap-

Nomenclature

$\bar{c}$ = chord length
c_p = specific heat of air at constant pressure
d = ejection hole diameter
$\bar{d}$ = exit hole diameter of the shaped hole
h_0, h = convective heat transfer coefficient without, with film cooling, $h = \dot{q}/(T_{0\infty} - T_w)$
i = incidence angle (positive in the counter clockwise direction)
k = thermal conductivity of air
l = Prandtl's mixing length, $l = [-u'v'/(\partial u/\partial y)]^{1/2}$
l_{max} = maximum of the mixing length augmentation for film cooling on the turbine blade
m = blowing rate
$\delta\dot{m}$ = coolant mass flow rate, shed into a stream tube
$\dot{m}_{old}$ = mass flow rate per unit depth in a stream tube
Ma = local Mach number
Nu_o = local Nusselt number, $Nu_o = h_0 \cdot s/k$
Pr = molecular Prandtl number, $Pr = \mu \cdot c_p/k$
PD = penetration depth
$\overline{PD}$ = constant penetration depth, $\overline{PD} = 0.8 \times \delta$
$\dot{q}$ = wall heat flux rate
Re = local Reynolds number, $Re = \rho_\infty U_\infty S/\mu_\infty$
$1/R$ = curvature
s = curvilinear distance on the suction side
St_0, St = Stanton number without, with film cooling ($St = h/\rho_\infty U_\infty C_p$)
T = temperature
TU = turbulence intensity $TU = \sqrt{\overline{u'^2}}/U$
U = velocity
u', v' = fluctuating velocity components
y = distance from the wall in a boundary layer
ρ = density
μ = absolute viscosity of air
δ = boundary layer thickness, $\delta_{.99}$
$\bar{\theta}$ = momentum thickness
κ = von Karman constant, $\kappa = 0.41$
θ = nondimensional coolant temperature,

$$\theta = \frac{T_{0\infty} - T_c}{T_{0\infty} - T_w}$$

η = adiabatic wall effectiveness

Subscripts

aw = adiabatic wall
$\bar{c}$ = based on chord length
c = relative to coolant
ex = exit
in = inlet
o = total condition
r = recovery
w = wall
∞ = relative to free stream
$\bar{\theta}$ = based on momentum thickness

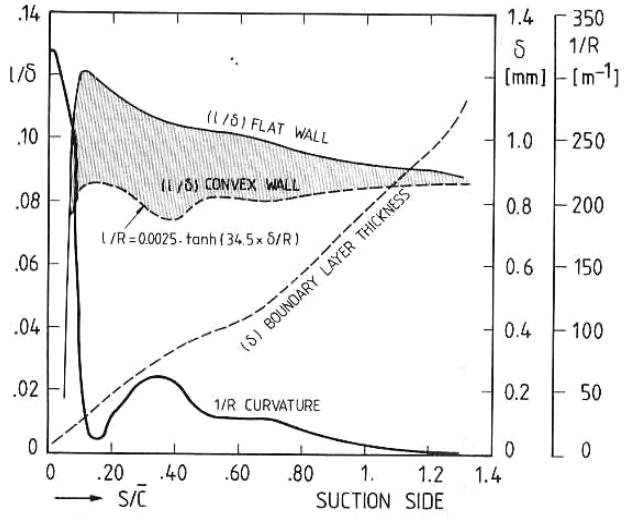

Fig. 3 Outer layer mixing length, curvature and boundary layer thickness on suction side

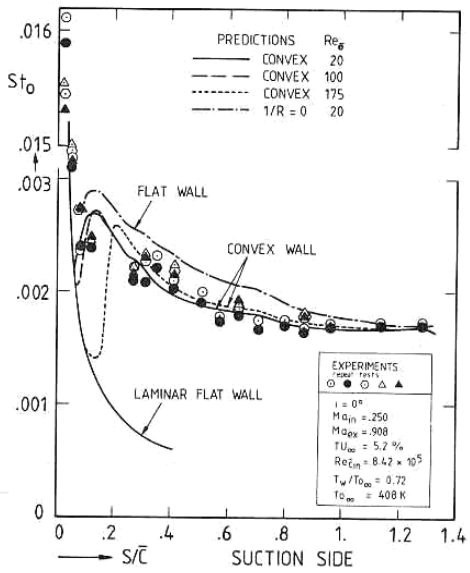

Fig. 4 Measured St_ϑ number distribution and predictions without cooling

pings and fast response thermocouples provided the coolant characteristics at the plenum inlet and outlet.

The local heat flux is deduced from the corresponding time-dependent surface temperature evolution, provided by the thin films. The temperature/wall heat flux conversion is obtained from an electrical analogy, simulating a one-dimensional, semi-infinite body configuration. A detailed description of this transient technique is given in [11, 12] and the measurement uncertainties were quoted in [13]. The convective heat transfer coefficient is defined as the ratio of the measured wall heat flux over the difference between free-stream recovery and local wall temperature; a recovery factor equal to 0.896 is used [13]. Flow temperatures are measured using fine tungsten wires (5–10 μm) and thermocouples (20 μm).

Suction-Side Heat Transfer Without Film Cooling, Measurements

Heat transfer behavior in the stagnation region of the present model and downstream boundary layer development have been investigated by the authors [13]. Compared to the model having an identical external contour but without cooling holes, an early laminar/turbulent transition is observed, due to the tripping effect of the leading edge cooling holes. A turbulent boundary layer is fully established for $s/\bar{c} > 0.2$. The existence of a fully turbulent boundary layer is confirmed by examining the timewise variation and the order of magnitude of the heat flux signal traces. As a consequence of the present investigation, the coolant film ejected from the suction-side holes always interacts with a fully turbulent boundary layer.

The local Nusselt number along the suction side, in the absence of coolant, has been plotted as a function of local Reynolds number (Fig. 2) and compared with the laminar and turbulent flat-plate correlations [14]. The reduction of turbulent shear stress and turbulent kinetic energy levels, especially in the outer layer of a turbulent boundary layer developing on a convex surface, are closely related with wall heating rate reductions [15]. The actual data indeed show somewhat lower values than the turbulent flat-wall correlation. The largest deviations are observed near the leading edge, where the transition is artificially induced by the holes which are not ejecting ($0.05 < s/\bar{c} < 0.2$). Further downstream, the measured values tend to merge with the flat-plate correlation as strong convex curvature disappears. A full recovery near the trailing edge is, however, not expected [16].

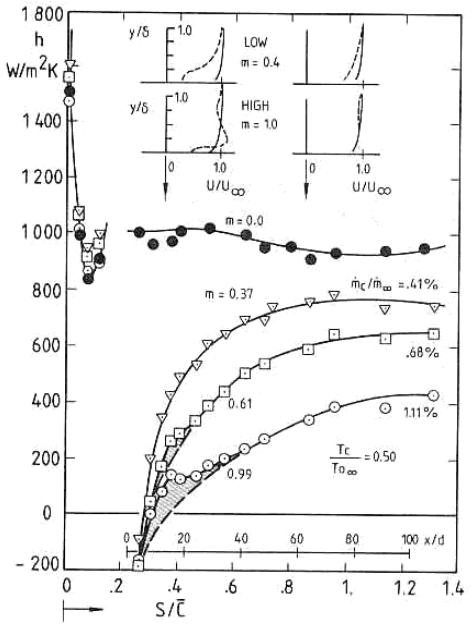

Fig. 5 Suction-side heat transfer with film cooling, effect of blowing rate

Suction-Side Heat Transfer Without Film Cooling, Predictions

A numerical prediction of convective heat transfer across the suction side has been attempted using a two-dimensional, finite difference boundary layer code (STAN5) developed by Crawford et al. [17]. The initial velocity and enthalpy profiles are obtained from a cylinder in crossflow solution. A streamwise curvature correction [16], based on mixing length modifications in the outer region of a turbulent boundary layer has been implemented in the code. This outer layer mixing length is computed from the equation shown in Fig. 3, using the local wall curvature. As a result, small l/δ values are obtained compared to a flat-plate configuration. In the log

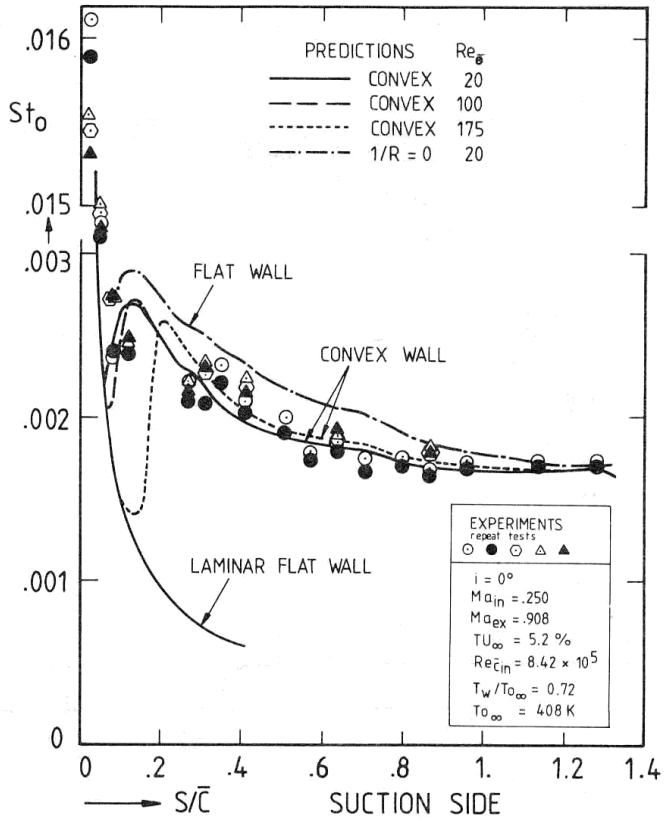

Fig. 4 Measured St_ϑ number distribution and predictions without cooling

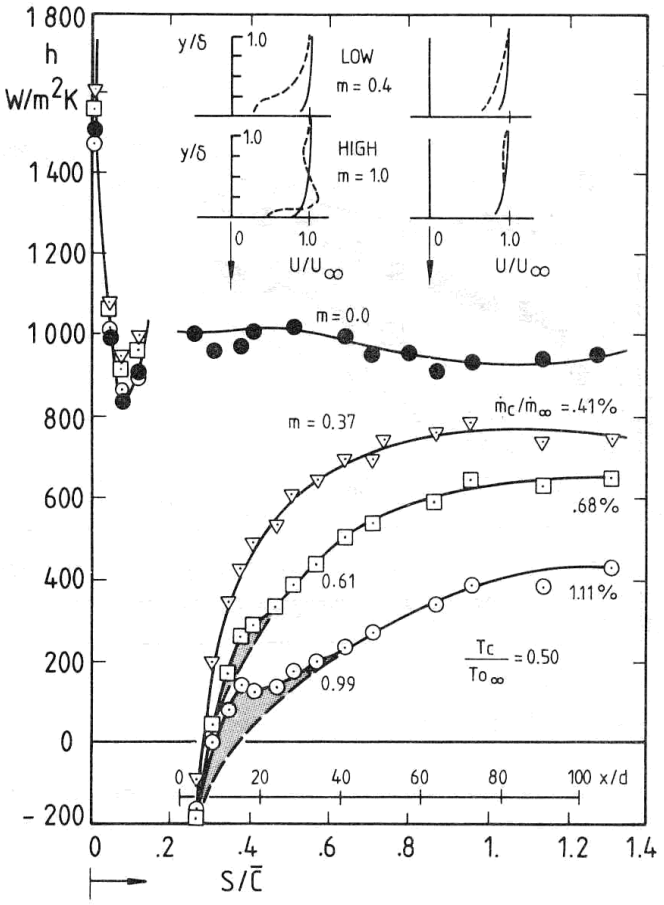

Fig. 5 Suction-side heat transfer with film cooling, effect of blowing rate

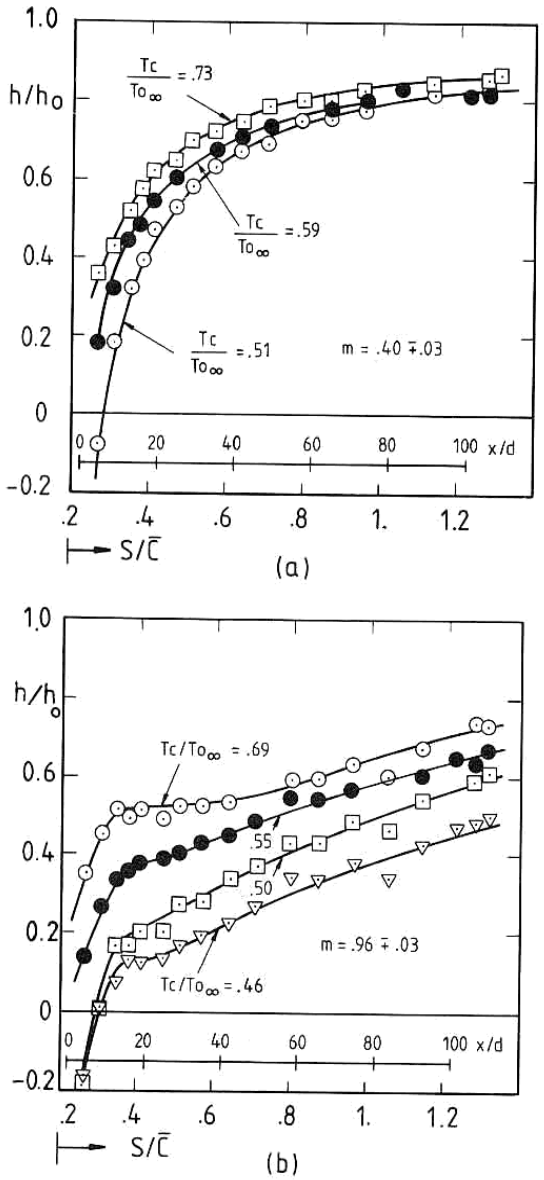

Fig. 6 Suction-side heat transfer with film cooling, effect of temperature ratio

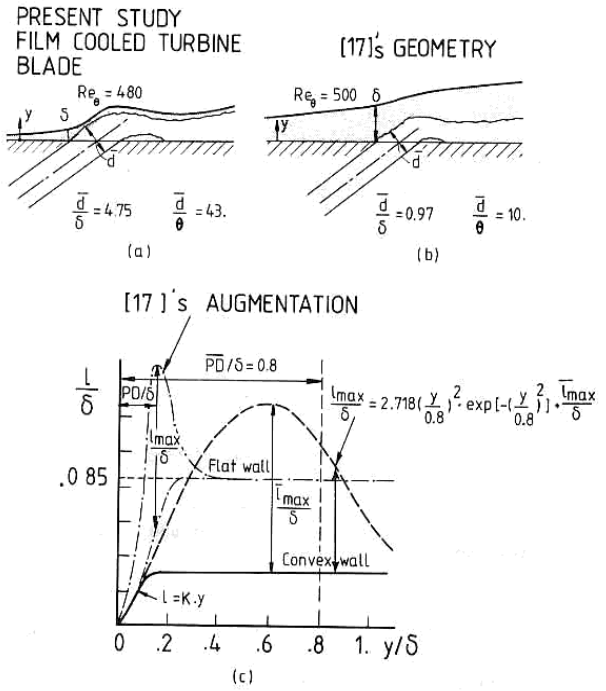

Fig. 7 Film-cooled boundary layer scaling on the turbine blade and mixing length augmentation

region, the shear stress correction was provided using a Richardson number formulation [16, 18]. As a matter of fact, for large convex curvature, the wall layer is structurally unchanged compared to a flat wall flow [16].

As already mentioned, an early boundary layer transition was forced by imposing a transitional Re_{θ} equal to 20 . . . 175. The predicted boundary layer thickness evolution is shown in Fig. 3. On the suction-side injection site, δ was computed to be 0.2 mm, i.e., almost five times smaller than a cooling hole diameter. Measured and computed local St_0 number distributions are compared in Fig. 4. These results clearly show the overprediction obtained without curvature correction and demonstrate the improvement obtained with a rather simple approach as the one presented above. Variations of transitional Re_{θ} between 20 . . . 175 . . .200 do not affect significantly the downstream convective wall heating rate level. The data scatter observed near the injection side is attributed to the disturbing influence of the relatively large diameter of cooling holes, although the injection plenum was filled with an insert.

Suction-Side Heat Transfer With Film Cooling, Measurements

Qualitative oil flow visualizations were performed in a low-speed environment; they demonstrated the spanwise uniformity of the coolant flow as well as the adequate film coverage, downstream of the ejection rows. It was also observed that the secondary flow region did not significantly affect the coolant field.

The influence of the blowing rate on the suction side convective heat transfer is shown in Fig. 5. The blowing rate was varied from 0.37 to 0.99 for a constant value of coolant to free-stream temperature ratio ($T_c/T_{0\infty} = 0.51$). In all cases, significant protection of the wall was achieved, especially close to the ejection holes, ($x/d < 40$). Typical velocity profiles, near and far downstream of double rows of holes, have been extracted from [19, 20] (Fig. 5). For low blowing rates ($m = 0.40$), low mean velocity gradients near the wall and important momentum deficits above $y/\delta = 0.2$ are typically encountered. If m is raised up to 1.0, a velocity excess region is observed near the wall. Above this zone, the overall mean velocity gradient is very low compared to the preceding configuration. Since the turbulent kinetic energy production is related to the mean velocity gradient [19], higher heat flux levels are expected for low blowing rates whereas, except in the near wall region, a reduction in overall heat flux will be observed for $m = 1.0$. In the near wall region, the heat transfer augmentation observed for $x/d < 40$ may be related to the velocity excesses shown in Fig. 5. Very steep mean velocity gradients near the wall as well as an eventual jet penetration into the mainstream yields large shear stress and turbulent kinetic energy levels in this region. For most of the aforementioned studies, the approaching mainstream boundary layer thickness δ has the same order of magnitude as the injection hole diameter. Although the mean velocity profiles provide a good aid in the interpretation of the data presented in Fig. 5, the δ/d ratio predicted for the present experiments is only 1/5, closer to a real situation. A

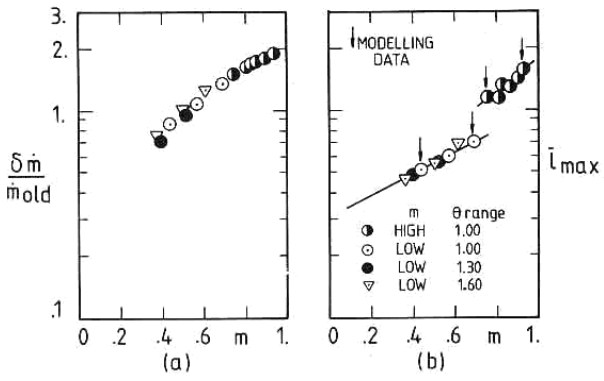

Fig. 8 Mass shed ratio and augmented mixing length

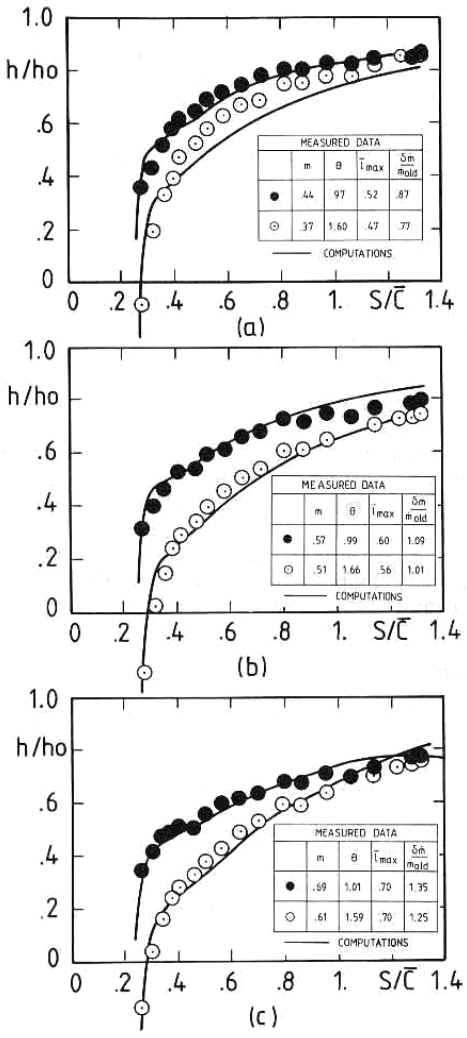

Fig. 9 Film cooling heat transfer, predictions $m < 0.69$

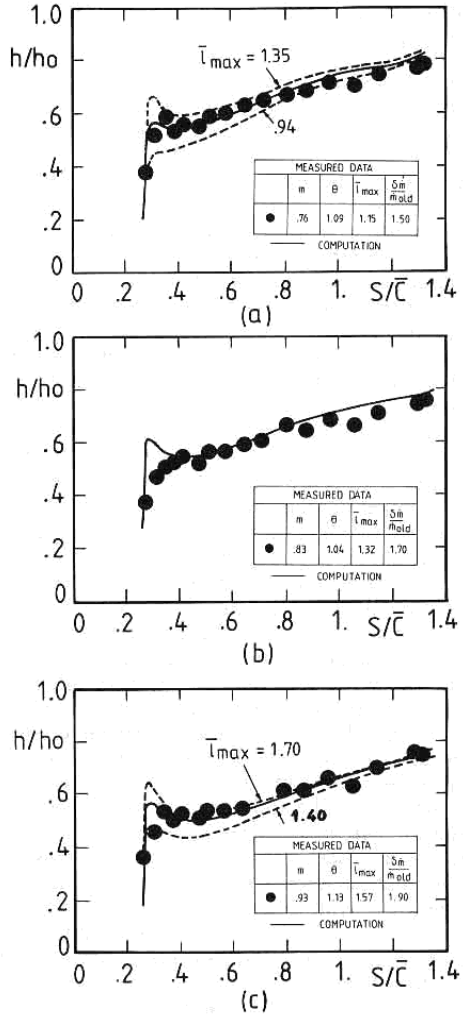

Fig. 10 Film cooling heat transfer, predictions $m > 0.76$

strong dominance of the new cold injected layers is therefore expected to take place.

Significant coolant temperature effects on convective heat transfer have also been observed. Figure 6(*a*) presents the results obttained for $m = 0.40$. Important h/h_0 reductions were achieved for $x/d < 40$ when the coolant temperature was lowered from wall temperature, to half of the mainstream level. The downstream values of h/h_0 smoothly increase and far downstream ($x/d = 100$) the heat flux level differences due to T_c variations are not as large as close to the ejection rows. Increasing m up to 0.96 provided the results presented in Fig. 6(*b*) with considerably lower heat transfer levels. Just downstream of the ejection side ($x/d < 40$), a local heat transfer augmentation, occurring almost independently of the coolant temperature level, is observed. This augmentation has been related to very high overall turbulent shear stress and turbulent kinetic energy levels near the wall, existing for such a blowing rate value. Another expected reason was "hot mainstream/wall" interaction due to severe coolant jet penetration into the mainstream. The penetrating coolant jets were expected to reduce the overall film cooling coverage just downstream of the ejection side, because of reduced lateral jet spread. In this zone, the wall has more chance to be influenced by the hot mainstream. Farther downstream, when the abrupt changes in the hydrodynamic structure start to decay, an almost linear h/h_0 rise takes place ($x/d = 30$). In contrast to the $m = 0.4$ case, the far downstream coolant temperature influence was very much pronounced. At $m = 0.96$, mainly because of considerably high momentum flux of the discrete coolant jets, the coolant layers tend to dominate even far downstream, as far as convective heat transfer is concerned.

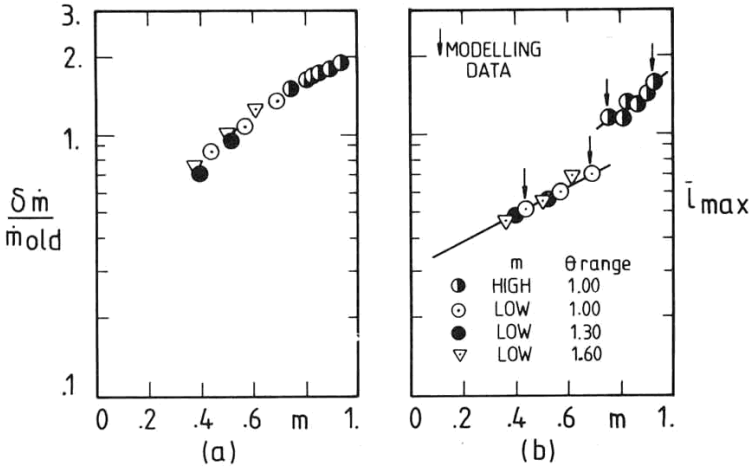

Fig. 8 Mass shed ratio and augmented mixing length

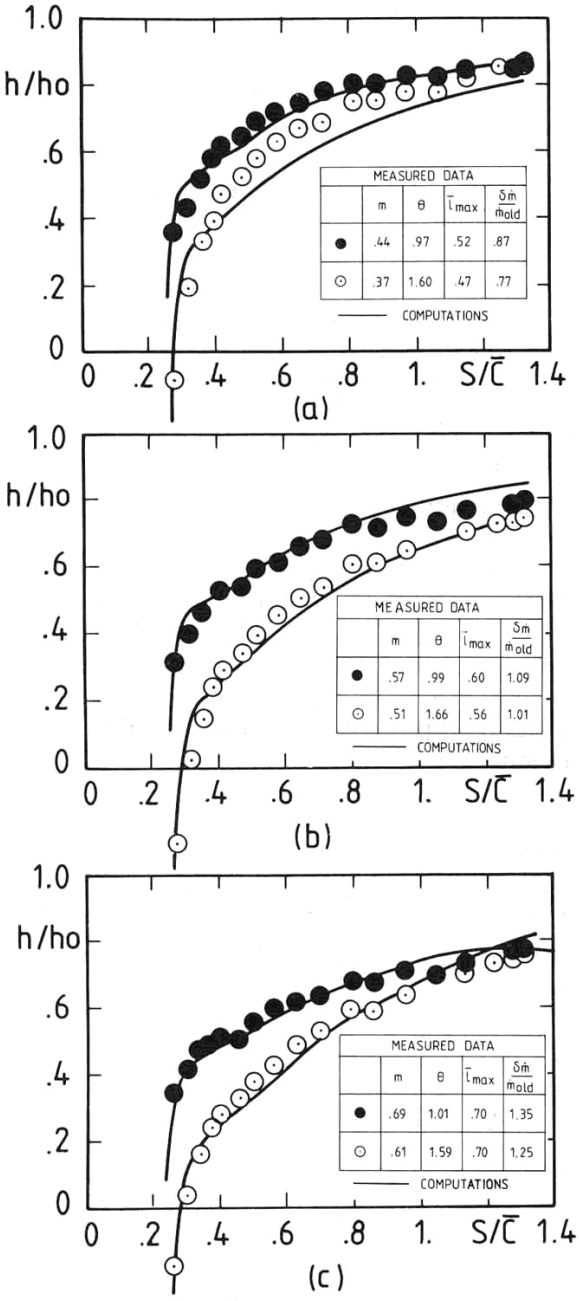

Fig. 9 Film cooling heat transfer, predictions $m < 0.69$

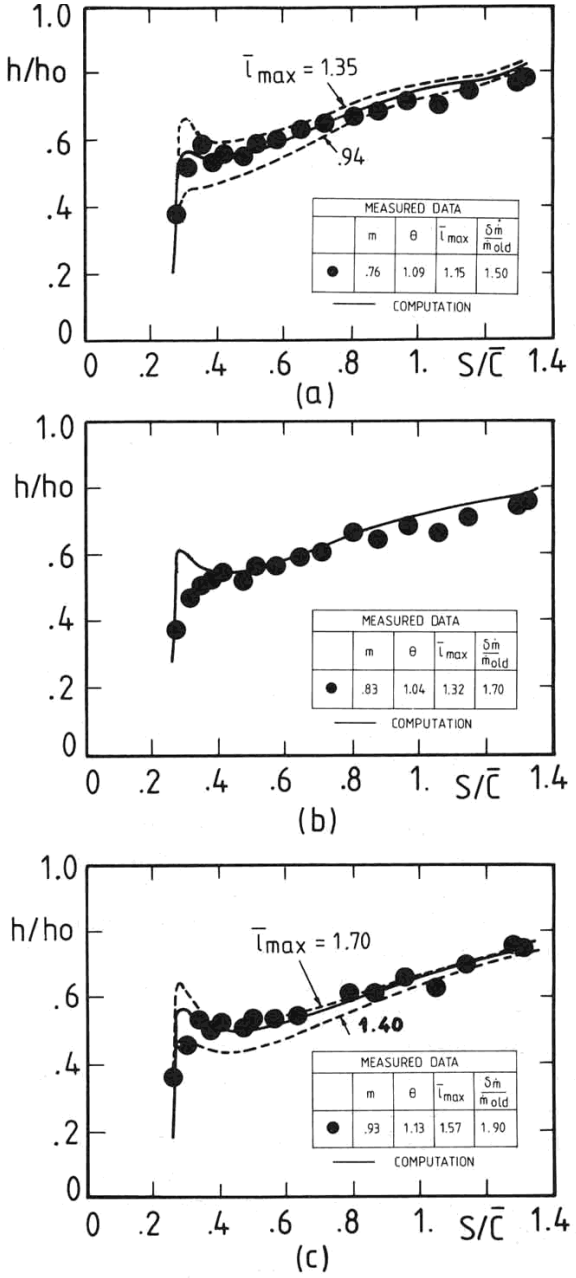

Fig. 10 Film cooling heat transfer, predictions $m > 0.76$

Suction-Side Heat Transfer With Film Cooling, Computations

The numerical simulation of convective heat transfer across the suction side in the presence of discrete hole film cooling was attempted using the boundary layer code developed for full coverage film cooling on flat walls by Crawford et al. [17]. Because of the existence of curved high-speed and compressible coolant layers along the suction side of the blade, a number of modifications, related to the effect of streamwise curvature as Prandtl's mixing length turbulence augmentation near the ejection holes and to the coolant ejection into the boundary layer, have been introduced.

The ejection hole diameter d to momentum thickness $\bar{\theta}$ ratio has been one of the basic simulation parameters in the area of discrete hole film cooling. In the present case, the $d/\bar{\theta}$ ratio was computed to be 43 whereas the d/δ ratio was calculated to be 4.75 (Fig. 7(a)). Looking at the model used in [17], values respectively equal to 10 and 1 were observed (Fig. 7(b)).

As a matter of fact, the coolant layers on the present model are expected either to occupy a major portion of the boundary layer or to penetrate into the mainstream and reattach farther downstream to the wall, depending upon the blowing rate level, in contrast to the case presented in [17], where the boundary layer is almost equally dominated by both mainstream and coolant flows. Therefore, the blowing rate dependency of the augmented mixing length $\bar{l}_{max}$ and mass shed ratio $\delta\dot{m}/\dot{m}_{old}$, the two most importrant parameters modeling the ejected flow, is strongly needed.

In order to establish the relationship existing between mass shed ratio and blowing rate, it was assumed that all of the coolant was distributed in such a way that the penetration depth did not exceed the approach boundary layer thickness. The resulting $\delta\dot{m}/\dot{m}_{old}$ values are shown in Fig. 8(a). Although this approach does not simulate the most accurate coolant distribution across the boundary layer, it is expected to simulate the overall hydrodynamic nature of the coolant layers downstream of the ejection site. At least this approach adds the correct amount of coolant mass and momentum to the viscous flow field.

The augmentation mixing length $\bar{l}_{max}$, representing the maximum disturbance to the boundary layer due to ejection, has been considered in the present study, as a lumped quantity, responsible for the gross mixing length modifications in the viscous layers. Moreover, the wall heat flux augmentation due to the "hot mainstream/wall" interaction described in the preceeding section was also expected to be simulated using this parameter, although no modifications were brought to the mass shed ratio. The exponential l_{max} variation used in [17] was found to be useful to simulate an augmentation which is spread over the entire boundary layer, with a *PD* located at 80 percent of the approaching boundary layer thickness, (Fig. 7(c)). $\bar{l}_{max}$ was decayed exponentially in the downstream direction with a time constant of two boundary layer thicknesses. Farther away from the ejection site the mixing length simulation takes only streamwise curvature effects into account.

The quantitative determination of $\bar{l}_{max}$ was performed by varying this quantity until a satisfactory simulation of the measured heat transfer data was obtained for two different blowing rates, (m = 0.44, 0.69) (Fig. 8(b)). The straight line connecting these two modeling $\bar{l}_{max}$ values was used in the predictions, for different blowing rates, at three different coolant temperatures, when $m < 0.69$. However, $\bar{l}_{max}$ was found to be independent of the coolant temperature in this range. The low blowing rate data were predicted successfully as presented in Fig. 9. However, this line was not very satisfactory in simulating the high blowing rate data ($m >$ 0.69). Starting from the idea of "hot mainstream/wall" interaction, which may occur above a certain blowing rate, another $\bar{l}_{max}$ region with a stronger m dependency was established using again two sets of measured data. The second $\bar{l}_{max}$ relation (Fig. 8(a)) was used successfully to predict six more data sets (m = .76, .81, .83, .86, .90, .93) for θ = 1.0. Three of the predictions are shown in Fig. 10. The agreement is good.

Conclusions

Convective heat transfer in the boundary layer developing along the suction side of a high-pressure turbine rotor blade has been investigated, both in absence and presence of film cooling, under well-simulated mainstream conditions and δ/d.

The experimental investigation was performed using a sophisticated short duration technique. The measured data on the turbine blade, in the absence of the coolant flow, were compared to classical flat-plate correlations in order to determine the influence of curvature on heat transfer.

In the presence of cooling, the effects of blowing rate and temperature ratio was successively investigated and discussed with the aid of published hydrodynamic data. Important local differences in convective heat transfer behavior were observed at low and high blowing rates.

The numerical predictions were obtained from the STAN5/STANCOOL boundary layer code, including a number of modifications taking into account mixing lengths on a highly curved surface with film cooling. In the absence of film cooling, a streamwise curvature correction, affecting only the turbulent boundary layer was implemented. The boundary layer transition on the suction side of the film-cooled blade was quite early and abrupt compared to that of the blade without cooling holes, under identical free-stream conditions. This phenomenon shows the significance of a curvature correction procedure on a film-cooled blade even without ejection.

A new approach was attempted to determine the augmented mixing length $\bar{l}_{max}$ for film cooling, through quantitative wall heat flux measurements near the ejection site. Low and high blowing rate behavior of $\bar{l}_{max}$ has been evaluated on a two zone $\bar{l}_{max}$ versus m map. In spite of the simplicity of this modeling idea, computed and measured results compare quite well in a rather large blowing rate and coolant temperature range.

References

1 Marchal, P., and Sieverding, C. H., "Secondary Flows Within Turbomachinery Bladings," Paper 11, in *Secondary Flows in Turbomachines*, AGARD CP 214, 1977, also VKI Preprint 1977-11.

2 Kestin, J., and Wood, R. T., "The Mechanism Which Causes Free-Stream Turbulence to Enhance Stagnation Line Heat and Mass Transfer," *Heat Transfer*, Vol. 2, Amsterdam, Elsevier, 1970.

3 Lander, R. D., Fish, R. W., and Suo, M., "External Heat Transfer Distribution on Film Cooled Turbine Vanes," *Journal of Aircraft*, Vol. 9, No. 10, Oct. 1972, pp. 707-714.

4 Muska, J. F., Fish, R. W., and Suo, M., "The Additive Nature of Film Cooling From Rows of Holes," ASME JOURNAL OF ENGINEERING FOR POWER, Vol. 98, No. 4, Oct. 1976, pp. 457-463.

5 Ito, S., Goldstein, R., and Eckert, E.R.G., "Film Cooling of a Gas Turbine Blade," ASME JOURNAL OF ENGINEERING FOR POWER, Vol. 100, No. 3, July 1978, pp. 476-481.

6 Dring, R. P., Blair, M. F., and Joslyn, H. D., "An Experimental Investigation of Film Cooling on a Turbine Rotor Blade," JOURNAL OF ENGINEERING FOR POWER, Vol. 102, No. 1, Jan. 1980, pp. 81-87.

7 Richards, B. E., Ville, J. P., Appels, C., and Salemi, C., "Film Cooling of Heated Turbine Surfaces at Simulated Conditions," Paper No. AIAA 77-947, AIAA/SAE 13th Joint Propulsion Conference, Florida, July 1977.

8 Consigny, H., and Richards, B. E., "Short Duration Measurements of Heat Transfer Rate to a Gas Turbine Blade," ASME JOURNAL OF ENGINEERING FOR POWER, Vol. 104, No. 3, July 1982, pp. 542-551.

9 Richards, B. E., "Heat Transfer Measurements Related to Hot Turbine Components in the von Karman Institute Hot Cascade Tunnel," in *Testing and Measurement Techniques in Heat Transfer and Combustion*, AGARD CP 281, 1980.

10 Jones, T. V., Schultz, D. L., and Hendley, A. D., "On the Flow in an Isentropic Free Piston Tunnel," ARC R&M 3731, Jan. 1973.

11 Schultz, D. L., and Jones, T. V., "Heat Transfer Measurements in Short Duration Hypersonic Facilities," AGARDograph 165, 1973.

12 Ligrani, P. M., Camci, C., and Grady, M.S., "Thin Film Heat Transfer Gauge Construction and Measurement Details," VKI TM 33, Nov. 1982.

13 Camci, C., and Arts, T., "Experimental Heat Transfer Investigation Around the Film-Cooled Leading Edge of a High-Pressure Gas Turbine Rotor Blade," paper to be presented at the ASME Gas Turbine Conf., Houston, Texas, March 17-21, 1985; also VKI Preprint 1984-32.

14 Kays, W. M., and Crawford, M. E., *Convective Heat and Mass Transfer*, (2d ed.), McGraw-Hill, 1980.

15 Gillis, J. C., and Johnston, J. P., "Turbulent Boundary Layer Flow and Structure of a Convex Wall and Its Redevelopment on a Flat Wall," *Journal of Fluid Mechanics*, Vol. 135, Oct. 1983, pp. 123-153.

16 Adams, E. W., and Johnston, J. P., "A Mixing Length Model for the Prediction of Convex Curvature Effects on Turbulent Boundary Layers," ASME JOURNAL OF ENGINEERING FOR GAS TURBINES AND POWER, Vol. 106, No. 1, Jan. 1984, pp. 142-148.

17 Crawford, M. E., Kays, W. M., and Moffat, R. J., "Full-Coverage Film Cooling. Part II: Heat Transfer Data and Numerical Simulation." ASME JOURNAL OF ENGINEERING FOR POWER, Vol. 102, No. 4, Oct. 1980, pp. 1006-1012.

18 So, R.M.C., "On the Curvature/Buoyancy Analogy for the Turbulent Shear Flows, *ZAMP*, Vol. 31, Fasc. 3, 1980.

19 Yavuzkurt, S., Moffat, R. J., Kays, W. M., "Full-Coverage Film Cooling. Part 1—Three-Dimensional Measurements of Turbulent Structure," *J. Fluid Mechanics*, Vol. 101, No. 1, Nov. 1980, pp. 120-158.

20 Bergeles, G., Gosman, A. D., and Launder, B. E., "Near-Field Character of a Jet Discharged Through a Wall at 30 deg to a Mainstream," *AIAA Journal*, Vol. 15, No. 4, Apr. 1977, pp. 499-504.

Printed in U.S.A.